HHS Public Access

Author manuscript

Retina. Author manuscript; available in PMC 2018 January 01.

Published in final edited form as:

Retina. 2017 January ; 37(1): 11–21. doi:10.1097/IAE.0000000000001250.

Ultrahigh Speed OCT Angiography of Retinal and Choriocapillaris Alterations in Diabetic Patients with and without Retinopathy Using Swept Source Optical Coherence Tomography

WooJhon Choi, PhD[1], **Nadia K. Waheed, MD**[2], **Eric M. Moult, BS**[1,3], **Mehreen Adhi, MD**[2], **ByungKun Lee, MS**[1], **Talisa De Carlo, BA**[2], **Vijaysekhar Jayaraman, PhD**[4], **Caroline R. Baumal, MD**[2], **Jay S. Duker, MD**[2], and **James G. Fujimoto, PhD**[1]

[1]Massachusetts Institute of Technology, Department of Electrical Engineering and Computer Science, and Research Laboratory of Electronics, Cambridge, MA

[2]Tufts University Medical Center, New England Eye Center, Boston, MA

[3]Harvard-MIT Division of Health Sciences and Technology, Cambridge, MA

[4]Praevium Research Inc., Santa Barbara, CA

Structured Abstract

PURPOSE—To investigate the utility of ultrahigh speed, swept source optical coherence tomography (SSOCT) angiography in visualizing retinal microvascular and choriocapillaris (CC) changes in diabetic patients.

METHODS—The study was prospective and cross-sectional. A 1050 nm wavelength, 400 kHz A-scan rate SSOCT prototype was used to perform volumetric optical coherence tomography angiography (OCTA) of the retinal and CC vasculatures in diabetic patients and normal subjects. 63 eyes from 32 normal subjects, 9 eyes from 7 PDR patients, 29 eyes from 16 NPDR patients, and 51 eyes from 28 diabetic patients without retinopathy were imaged.

RESULTS—Retinal and CC microvascular abnormalities were observed in all stages of diabetic retinopathy. In NPDR and PDR, OCTA visualized a variety of vascular abnormalities including: clustered capillaries, dilated capillary segments, tortuous capillaries, regions of capillary dropout, reduced capillary density, abnormal capillary loops, and foveal avascular zone enlargement. In PDR, retinal neovascularization above the inner limiting membrane was visualized. Regions of CC flow impairment in patients with PDR and NPDR were also observed. In 18 of the 51 of eyes from diabetic patients without retinopathy, retinal mircrovascular abnormalities were observed and CC flow impairment was found in 24 of the 51 diabetic eyes without retinopathy.

Corresponding Author/Reprint Requests. Correspondence to James G. Fujimoto, PhD, Department of Electrical Engineering and Computer Science, and Research Laboratory of Electronics, Massachusetts Institute of Technology, 77 Massachusetts Avenue, 36-345, Cambridge, MA 02139, jgfuji@mit.edu.

Meeting Presentation

Results presented in part at: Association for Research in Vision and Ophthalmology meeting, May 2014, Orlando, Florida.

CONCLUSIONS—The ability of OCTA to visualize retinal and CC microvascular abnormalities suggests OCTA may be a useful tool for understanding pathogenesis, evaluating treatment response, and earlier detection of vascular abnormalities in patients with diabetes.

Summary Statement

Swept source OCT angiography visualizes retinal and choriocapillaris microvasculature alterations in diabetic patients with and without retinopathy.

Keywords

angiography; choriocapillaris; diabetic retinopathy; optical coherence tomography (OCT); optical coherence tomography angiography (OCTA); retinal vasculature

Introduction

Diabetic retinopathy (DR), a complication of diabetes mellitus (DM), is the leading cause of vision loss amongst working age adults in developed countries.[1–3] Both retinal and choroidal blood circulations are altered in eyes with DR.[4–22] Multiple vascular abnormalities have the potential to be early markers of DR. Non-proliferative diabetic retinopathy (NPDR) is characterized by capillary pericyte loss, basement membrane thickening, and smooth muscle cell loss leading to the formation of microaneurysms,[4–10] which are important markers that predict DR progression.[11, 12] Moreover, foveal avascular zone (FAZ) enlargement and capillary dropout have been observed in fluorescein angiography (FA) studies in patients with early DR.[13–15, 22] More recently, OCT angiography (OCTA) studies have demonstrated the presence of microanueurysms and capillary dropout in patients with diabetic retinopathy.[23] Although DR is generally considered to be a disease of retinal vessels, histology, electron microscopy, and FA and indocyanine green angiography (ICGA), studies have shown diabetes to be associated with choriocapillaris (CC) degeneration as well as basal laminar deposit formation; the term *diabetic choroidopathy* has been used to refer to CC alterations associated with diabetes.[16–20, 24–27]

Imaging of the retinal and choroidal vasculatures in diabetic patients is not routinely performed, especially for patients at an early stage of DR, since conventional dye-based angiography techniques, such as FA and ICGA, require intravenous administration of exogenous dyes. Moreover, because of its location and structure, visualization of the CC is challenging with both FA and ICGA.[28, 29] OCTA is a relatively new imaging technique that enables noninvasive volumetric visualization of the retinal and CC vasculatures.[30–34] OCTA is based on motion contrast and, unlike FA and ICGA, does not require the injection of exogenous dyes. An OCTA B-scan is generated by acquiring repeated OCT B-scans acquired in rapid succession from the same retinal location. If the tissue is stationary, the repeated B-scans will be identical; however, if there is blood flow, the moving erythrocytes will cause pixels in the repeated OCT B-scans to become decorrelated by an amount related to the flow speed. An OCTA volume can be generated by acquiring repeated B-scan sets at multiple retinal locations. Because OCT is depth resolved, different retinal and choroidal vascular layers can be separately visualized, a feature that is not possible with dye-based angiography.[35–38] Moreover, since it is noninvasive, OCTA can be repeated multiple times

on subsequent visits, or even during the same visit. Finally, since OCTA is an extension of standard OCT imaging, structural information is obtained at the same time, and is intrinsically co-registered to angiographic information. This feature enables simultaneous visualization of both structural and angiographic data.

Compared to structural OCT, OCTA requires higher imaging speeds because of the repeated B-scan protocol. Consequentially, until the recent introduction of high speed OCT systems, the clinical usage of OCTA has been limited. In 2012, Kim et al. demonstrated imaging of the FAZ of 2 healthy subjects and 8 diabetic patients using OCTA.[39] In 2014, Schwartz et al. reported OCTA imaging results from 1 normal subject and 1 NPDR patient.[40] More recently, Ishibazawa et al. studied a larger cohort of 25 diabetic patients using a commercially available spectral-domain system and showed that OCTA is able to visualize microaneurysms and retinal nonperfused areas in diabetic retinopathy.[41]

In this study, we investigate the potential of ultrahigh speed, 1050 nm swept source OCT (SSOCT) as a modality to visualize changes in the retinal and CC vasculatures in diabetic patients at different stages of DR and in diabetic patients without clinical retinopathy. The vasculatures of diabetic patients are also compared to those of healthy, control eyes.

Methods

This study protocol was approved by the Institutional Review Boards at the Massachusetts Institute of Technology (MIT) and Tufts Medical Center. All participants were imaged in the ophthalmology clinic at the New England Eye Center (NEEC) and written informed consent was obtained prior to imaging. The research adhered to the Declaration of Helsinki and the Health Insurance Portability and Accountability Act.

The study was prospective and cross-sectional. All subjects underwent a complete ophthalmic examination including a detailed history, refraction, intraocular pressure measurement, anterior segment examination and a dilated fundus examination by an ophthalmologist at the NEEC. Diabetic patients received color fundus photography and FA as clinically indicated. Normal (control) subjects were defined as having a normal ophthalmic examination except for age-appropriate cataracts, normal visual fields, refraction less than or equal to 6D, and no history of diabetes. Patients with Type 1 or Type 2 diabetes without any retinopathy documented on a detailed dilated ophthalmic exam by a retinal specialist were classified as diabetic patients without retinopathy. Diabetic patients with retinopathy were classified, into nonproliferative and proliferative diabetic retinopathy based on a clinical evaluation of the patient. This was validated by comparison with fundus photos where available. The classification into no diabetic retinopathy, nonproliferative diabetic retinopathy, and proliferative diabetic retinopathy was found to be reproducible between the clinician impression and a formal Early Treatment of Diabetic Retinopathy Study (ETDRS) grading of the fundus photograph, where available, by two trained readers at the Boston Image Reading Center.

OCTA was performed using an investigational ultrahigh speed SSOCT research prototype developed at MIT and in use at NEEC. A similar OCT system was described previously[42]

and therefore only key characteristics are summarized herein. The prototype OCT instrument uses a vertical cavity surface emitting laser (VCSEL) swept light source with a 400 kHz A-scan rate. The light source is centered at 1050 nm wavelengths which, when compared to the 840 nm wavelengths used in most commercial systems, enables deeper light penetration into the RPE, choroid, and reduced attenuation from ocular opacities.[43] OCT interferometric signals are acquired with an analog-to-digital acquisition card externally clocked at a maximum frequency of ~1.1 GHz using an external Mach-Zehnder interferometer.

OCTA imaging was performed with 6 mm × 6 mm and 3 mm × 3 mm fields of view. For both field sizes, 5 repeated B-scans from 500 uniformly spaced locations were sequentially acquired. Each B-scan consisted of 500 A-scans and the interscan time between repeated B-scans was ~1.5 ms, accounting for the mirror scanning duty cycle. The acquisition time for repeated B-scans was ~7.5 ms (~1.5 ms × 5) per position. A total of 5 × 500 × 500 A-scans were acquired per OCTA volume for a total acquisition time of ~3.9 s. The volumetric scan pattern yields isotropic transverse sampling of the retina at 12 μm and 6 μm intervals for the 6 mm × 6 mm and 3 mm × 3 mm field sizes, respectively. Smaller field sizes have proportionately more transverse sample density and provide higher OCTA image quality.

OCTA images were generated by calculating a decorrelation signal on a pixel-by-pixel basis between sequential OCT B-scans (1↔2, 2↔3, 3↔4, and 4↔5) acquired from the same location with a ~1.5 ms interscan time. To correct for eye motion, which produces spurious decorrelation signals, the repeated B-scans were motion corrected using a rigid registration algorithm prior to calculating decorrelation.[44] For each B-scan location, the 4 resulting decorrelation images were averaged to improve the signal-to-noise ratio. This was performed at all 500 B-scan locations in order to obtain a three-dimensional OCTA volume.

There are 4 vascular plexuses in the macular area: the vascular plexus in the nerve fiber layer (NFL); the vascular plexus in the ganglion cell layer (GCL) and superficial portion of the inner plexiform layer (IPL); the vascular plexus in the deep portion of the IPL and superficial portion of the inner nuclear layer (INL); and the vascular plexus in the deep portion of the INL.[45] For this study we grouped the vascular plexuses of the NFL and the GCL together, which is termed the superficial plexus; the vascular plexus of the deep portion of the IPL and superficial portion of the INL is termed the intermediate plexus; and the vascular plexus in the deep portion of the INL is termed the deep plexus. The NFL and GCL plexuses were grouped together because they were difficult to accurately separate. When forming en face OCTA images of the retinal vasculature, the OCTA volume was either mean projected through individual vascular plexuses, or through all retinal plexuses. To better visualize the vasculature, as a final processing step, certain en face OCTA projections were manually motion corrected—such images are noted as being manually motion corrected in their corresponding figure's legend. Manual motion correction was performed by "cutting" en face projections along the lines corresponding to patient motion. This cutting operation decomposed the en face images into a number of strips, which were then manually aligned by translation—here, vascular continuity was used to as a metric of alignment. The manual motion correction process typically took between 5–10 minutes per image, depending on the number of motion artifacts present. When performing measurements of the FAZ, a total

retinal projection—i.e., a projection through the depths spanned by all retinal plexuses—was used. En face OCTA CC slabs were generated by selecting a single en face plane, ~4.4 μm in thickness, immediately below Bruch's membrane. The 4.4 μm slice thickness is a result of dividing the imaging range by the number of acquired samples.

Results

A total of 63 eyes from 32 normal subjects, 9 eyes from 7 PDR patients, 29 eyes from 16 NPDR patients, and 51 eyes from 28 diabetic patients without retinopathy were imaged for this study (Table 1).

Normal subjects

The normal subjects had a mean age (± SD) of 40.7 ± 14.1 years (range: 19 to 70 years; 63 eyes of 32 participants). Among the 63 eyes imaged, 33 were from subjects 40 years or older and 7 were from subjects 60 years or older. In general, we found that the 3 mm × 3 mm field size better visualizes vascular details due to the higher A-scan sampling density as compared to the 6 mm × 6 mm field size.

Representative en face OCTA images of the three different plexuses in a normal subject are shown in Figure 1B–1D. The retinal capillary network was generally dense in all normal subjects; none of the retinal capillary networks from the normal eyes had the degree of tortuosity observed in the diabetic eyes (described below). The mean (± SD) FAZ diameter measured in the longest dimension in normal eyes was 575 ± 146 μm. Two eyes from the same subject were treated as being independent. Although slight variations in the CC density were observed, the CC of normal subjects was generally dense and homogeneous (Figure 1E).

Proliferative diabetic retinopathy

The PDR cohort had a mean age (± SD) of 51.4 ± 16.3 years (range: 26 to 67 years; 9 eyes of 7 participants). Of the 9 eyes, 8 eyes were treated previously with panretinal photocoagulation, and 3 eyes were treated with anti-vascular endothelial growth factor (anti-VEGF) for associated macular edema. In eyes with PDR, the retinal capillary density was lower and the capillaries more tortuous compared to normal eyes. In addition, FAZ contours were asymmetric due to capillary dropout at the borders of the FAZ. The mean (± SD) FAZ diameter in the longest dimension in eyes with PDR was 1150 ± 165 μm. Retinal vasculature abnormalities, including dilated capillary segments, tortuous capillaries, capillary dropouts, reduced capillary density, capillary loops, and/or enlarged FAZ were readily visible in all 9 eyes with PDR. Select PDR cases are shown in Figure 2. In the situations where the retinal neovascularization was visible within the OCTA imaging field, it occurred above the ILM, as shown in Figure 2B–2C.

Varying degrees of CC alteration were also observed in PDR eyes. The en face OCTA CC slabs in Figure 2E–2I demonstrate CC flow impairment. In some cases, CC flow impairment was more pronounced in localized areas (Figure 2E), while in other cases, it was diffusely distributed throughout the field of view (Figure 2G). In 2 of the eyes, CC flow was severely impaired and large choroidal vessels were visible (Figure 2I), although the choroidal

thickness was in the normal range. Some degree of CC flow impairment was observed in 7 of the 9 PDR eyes.

Nonproliferative diabetic retinopathy

The NPDR cohort had a mean age (± SD) of 60.8 ± 7.4 years (range: 45 to 73 years; 29 eyes of 16 participants). 27 of the 29 eyes with NPDR demonstrated retinal microvascular abnormalities including microaneurysms, capillary dropout, FAZ enlargement and clustered/tortuous capillaries. Focal and/or diffuse CC alteration was observed in 15 of the 29 eyes with NPDR. Although retinal microvascular abnormalities were observed in all vascular plexuses, abnormalities were best visualized when the individual retinal vascular layers were separated. Capillary loops corresponding to microaneurysms were most often observed in the intermediate plexus, while capillary dropout and severely tortuous capillary branches best observed in the superficial plexus.

Figure 3 shows a fundus photograph, en face OCTA of retinal vasculature (formed by projecting through all retinal plexuses), OCT retinal thickness map, and an en face OCTA CC slab from a 51 year old NPDR patient with diabetic macular edema (DME). The OCT retinal thickness map shows the location of edema (Figure 3C). In the en face OCTA of retinal vasculature, small capillary loops and abnormally tortuous capillary branches are visible in the regions near capillary dropout. Although retinal microvascular abnormalities visible in OCTA do not necessarily predict the location of edema, these microvascular abnormalities were frequently present near the regions of densely distributed cysts in DME.

The longest dimension of the FAZ in NPDR patients had a mean length (± SD) of 813 ± 208 μm. Similar to the PDR eyes, some CC flow impairment was noted in 15 out of 29 eyes with NPDR. The OCTA CC slab of the patient in Figure 3 is generally dense and homogenous. However, a small number of focal areas of CC flow impairment (white arrows) are visible in the field of view. In 2 of the eyes with NPDR (and one PDR eye), inner retinal layer thinning was correlated with patches of retinal capillary flow impairment. Although the 3 cases of inner retinal layer thinning were all associated with retinal capillary flow impairment, flow impairment did not necessarily involve inner retinal layer thinning.

En face OCTA images from 3 NPDR patients are shown in Figure 4. Note that vascular abnormalities are more evident when different retinal capillary plexuses are visualized separately.

Diabetes without retinopathy

Diabetic patients without retinopathy had a mean age (± SD) of 59.7 ± 13.2 years (range: 26 to 83 years; 51 eyes of 28 participants). Figure 5 shows 4 representative cases of diabetic eyes without retinopathy. In order to better visualize the vascular abnormalities, en face OCTA images of the superficial, intermediate, and deep plexuses as well as those of the entire retinal vasculature are shown. Figures 5E, 5J, 5O, and 5T show the corresponding OCTA CC slabs. The retinal and CC abnormalities observed in PDR and NPDR patients were also observed in a subset of diabetic patients without retinopathy, albeit with a generally reduced severity. The patient shown in Figures 5A–5E exhibits abnormally tortuous retinal capillary branches, retinal capillary dropout, and capillary loops around the

FAZ. The patient shown in Figures 5F–5J exhibits tortuous retinal capillary branches and severe capillary dropout, which are more evident when different capillary plexuses are visualized separately. The patient shown in Figures 5K–5O exhibits abnormally tortuous retinal capillary branches, retinal capillary dropouts, and severe focal CC flow impairment. The patient shown in Figures 5P–5T exhibits reduced capillary perfusion in the deep plexus and diffuse CC impairment. As shown in Figures 5A–5E and 5F–5J, abnormalities in the retinal vasculature did not always accompany CC flow impairment in this subgroup of patients, nor did the severity of the CC flow impairment obviously correlate with the severity of retinal vasculature abnormalities. For example, although the patient shown in Figures 5F–5J exhibits more retinal microvasculature abnormalities than the patient shown in Figures 5P–5T, CC impairment is more severe in the patient shown in Figures 5P–5T.

The mean (± SD) FAZ diameter in the longest dimension in diabetic patients without retinopathy was 696 ± 153 μm. Retinal microvascular abnormalities, such as capillary dropout, dilated capillary loops, tortuous capillary branches, patches of reduced capillary perfusion, irregular FAZ contours, and/or FAZ enlargement, were observed in 18 of the 51 diabetic eyes without retinopathy. Focal or diffuse CC flow impairment was also observed in 24 of the 51 diabetic eyes without retinopathy.

Discussion

OCTA using a prototype 400 kHz, 1050 nm wavelength SSOCT revealed abnormalities of the retinal vasculature as well as CC alterations in eyes with PDR and NPDR. These abnormalities were more severe and more frequent in eyes with PDR versus those with NPDR. The retinal vasculature changes included capillary dropout, dilated capillary loops, tortuous capillary branches, irregular FAZ contour and FAZ enlargement relative to normal subjects. These observations are consistent with those from previous studies performed using FA and OCTA.[13–15,22, 34, 41, 42]

To the authors' knowledge, the CC flow impairment in PDR and NPDR patients has not been described previously using OCTA. However, this finding is consistent with previous histology, electron microscopy, and FA and ICGA studies describing diabetic choroidopathy.[16–20, 24–27] OCTA enables visualization of the CC, which is challenging using conventional dye-based angiography techniques. The need for careful interpretation of CC OCTA images is, however, underscored by the variation seen among normal subjects. This variation led us to consider a diabetic patient's CC as abnormal only if the CC exhibited pronounced flow impairment relative to normal subjects, or if it showed pronounced inhomogeneity in the microvascular density over the OCTA field of view. There was no obvious spatial correlation between CC alteration and RPE/photoreceptor integrity in most diabetic eyes. In addition, the severity of retinal microvasculature and CC alteration were not obviously correlated.

Although post mortem studies report CC alterations in DR, the role of CC in diabetic retinopathy is incompletely understood.[16–20] In this study, CC alterations were common not only in PDR and NPDR, but also in diabetics without retinopathy, albeit with a generally reduced severity. This finding suggests that CC alterations also occur early in diabetes and

may play a role in the pathogenesis of DR. CC flow impairment at different stages of diabetic retinopathy merits further investigation.

This study also found abnormalities in the retinal vasculatures in diabetic subjects without clinical DR. This is consistent with previous findings suggesting vascular changes begin early in diabetes. A previous study using scanning laser video fluorescein angiography showed reduced capillary density in the perifoveal area of diabetics without retinopathy, consistent with our observation of capillary dropout in some diabetics without retinopathy.[22] It is possible that, together with the observed CC alterations, these retinal vasculature alterations, as opposed to microanuerysm formation, represent the earliest changes associated with NPDR.

OCTA has the advantage that it enables three dimensional visualization of retinal microvasculature at different depths. In diabetic eyes, we found that viewing the superficial, intermediate, and deep plexuses individually improved visualization of vascular abnormalities (Figure 4 and Figure 5). By projecting all retinal layers together, the vasculature may appear too dense, and obfuscate microvascular abnormalities. In this study, capillary loops or microaneurysms were most often visualized in the intermediate plexus, which is consistent with previous post mortem studies.[21, 46] In the superficial plexus, capillary dropout and severely tortuous capillary branches were the most frequently observed abnormalities. However, we could not determine whether vascular abnormalities were more severe in one vascular plexus vs another. We believe that visualization of the separate retinal vasculatures merits further investigation and may be an important tool in screening diabetic patients for earlier detection of microvascular abnormalities.

Unlike dye-based angiography techniques, OCTA does not visualize dye leakage. Although this can be a limitation for assessing vascular permeability, it can also be an advantage because fluorescence can obscure features. Moreover, the intrinsic registration of OCTA with OCT structural images and thickness maps, enables us to infer leakage from the microaneurysms in close proximity to retinal edema or retinal cysts and vascular integrity of microaneurysms that are not associated with retinal edema. OCTA enables direct three-dimensional visualization of abnormal vasculature and may therefore serve as a sensitive and direct approach for monitoring treatment response. For example, in DR, OCTA directly visualizes the microvasculature of microaneurysms as well as capillary dropout. However, not all microaneurysms visible on FA are detectable on OCTA, and vice versa.

A potential advantage of ultrahigh speed, swept source OCTA is that it can enable wider retinal coverage or higher sample density in comparison to commercially available spectral-domain OCTA instruments. This is especially important in diabetes where the microvascular changes are not confined to the macular area. That said, in this study we primarily focused on 3 mm × 3 mm fields of view, rather than larger 6 mm × 6 mm fields of view, because the increased transverse sampling density enabled better visualization of retinal microvasculature.

A limitation of this study is that the normal (control) subjects were not age-matched to the diabetic patients, although the range of normal subject ages was wide. Because the normal

subjects were, on average, younger than the diabetic patients, it is possible that some of the observed differences between the control group and the diabetic patients were due to, or accentuated by, ageing effects. Nevertheless, this study provides new information on CC alterations that occur in diabetic retinopathy as well as diabetics without retinopathy. In addition, the study shows that retinal microvascular changes occur in diabetics without retinopathy and are possibly a precursor to NPDR and PDR. Since OCTA imaging is noninvasive, it can be performed in diabetic patients where FA would not be indicated. Hence, ultrahigh speed, swept source OCTA may be a useful tool for earlier detection of microvascular abnormalities, elucidating pathogenesis, monitoring treatment response, and pharmaceutical development in patients with diabetes. The development of image processing and feature recognition algorithms which can quantitatively assess microvascular changes is an important area of future investigation. OCTA can be rapidly acquired and ultimately can be automatically graded without reader intervention. These imaging methods could provide a low cost, high throughput adjunct to methods such as the ETDRS grading. Quantitative measurement of microvascular changes would be important tool for assessing disease progression and response to therapy.[47] Changes in retinal or CC microvasculature may be a surrogate for the systemic vascular changes that occur in diabetes.

Acknowledgments

Financial Support

This work was supported by the National Institute of Health (NIH R01-EY011289-28, R44-EY022864-03, R01-CA075289-17), Air Force Office of Scientific Research (AFOSR FA9550-10-1-0551 and FA9550-12-1-0499), and Thorlabs matching funds to Praevium Research Inc. Additional support from an unrestricted Research to Prevent Blindness grant and the Massachusetts Lions Clubs, a Samsung Scholarship, and a Natural Sciences and Engineering Research Council of Canada Scholarship.

Financial Disclosure

The authors have made the following disclosures:

J.S. Duker - Research support from Carl Zeiss Meditec Inc. and Optovue Inc., and Topcon Medical Systems Inc.; and stock in Hemera Biosciences Inc., EyeNetra, and Ophthotech Corp.

J.G. Fujimoto - Royalties from intellectual property owned by Massachusetts Institute of Technology and licensed to Carl Zeiss Meditec Inc. and Optovue Inc., and stock options with Optovue Inc.

V. Jayaraman - Stock and employment at Praevium Inc., Royalities from Thorlabs Inc.

The authors wish to thank Dr. Ricardo Louzada, Dr. Eduardo Novais, and Emily Cole for their assistance in characterizing the subjects of this study.

References

1. Engelgau MM, Geiss LS, Saaddine JB, et al. The evolving diabetes burden in the United States. Annals of Internal Medicine. 2004; 140:945–950. [PubMed: 15172919]
2. Thylefors B, Négrel AD, Pararajasegaram R, et al. Global data on blindness. Bulletin of the World Health Organization. 1995; 73:115–121. [PubMed: 7704921]
3. Thylefors B. A global initiative for the elimination of avoidable blindness. Community Eye Health. 1998; 11:1–3. [PubMed: 17492014]
4. Cogan DG, Kuwabara T, Toussaint D. Retinal vascular patterns: IV. Diabetic retinopathy. Archives of Ophthalmology. 1961; 66:366–378. [PubMed: 13694291]

5. Cogan DG, Kuwabara T. Capillary shunts in pathogenesis of diabetic retinopathy. Diabetes. 1963; 12:293–300. [PubMed: 14081839]
6. Kuwabara T, Cogan DG. Retinal vascular patterns: VI. Mural cells of retinal capillaries. Archives of Ophthalmology. 1963; 69:492–502. [PubMed: 13927676]
7. Toussaint D, Dustin P. Electron microscopy of normal and diabetic retinal capillaries. Archives of Ophthalmology. 1963; 70:96–108. [PubMed: 13993857]
8. Speiser P, Gittelso A, Patz A. Studies on diabetic retinopathy: III. Influence of diabetes on intramural pericytes. Archives of Ophthalmology. 1968; 80:332–337. [PubMed: 4174771]
9. Hammes HP, Lin JH, Renner O, et al. Pericytes and the pathogenesis of diabetic retinopathy. Diabetes. 2002; 51:3107–3112. [PubMed: 12351455]
10. Roy S, Ha J, Trudeau K, et al. Vascular basement membrane thickening in diabetic retinopathy. Current Eye Research. 2010; 35:1045–1056. [PubMed: 20929292]
11. Klein R, Meuer SM, Moss SE, et al. Retinal microaneurysm counts and 10-year progression of diabetic-retinopathy. Archives of Ophthalmology. 1995; 113:1386–1391. [PubMed: 7487599]
12. Sjolie AK, Klein R, Porta M, et al. Retinal microaneurysm count predicts progression and regression of diabetic retinopathy. Post-hoc results from the DIRECT Programme. Diabetic Medicine. 2011; 28:345–351. [PubMed: 21309844]
13. Bresnick GH, Condit R, Syrjala S, et al. Abnormalities of the foveal avascular zone in diabetic-retinopathy. Archives of Ophthalmology. 1984; 102:1286–1293. [PubMed: 6477244]
14. Mansour AM, Schachat A, Bodiford G, et al. Foveal avascular zone in diabetes-mellitus. Retina-the Journal of Retinal and Vitreous Diseases. 1993; 13:125–128.
15. Arend O, Wolf S, Remky A, et al. Perifoveal microcirculation with non-insulin-dependent diabetes-mellitus. Graefes Archive for Clinical and Experimental Ophthalmology. 1994; 232:225–231.
16. Fryczkowski AW, Hodes BL, Walker J. Diabetic choroidal and iris vasculature scanning electron microscopy findings. Int Ophthalmol. 1989; 13:269–279. [PubMed: 2482264]
17. McLeod DS, Lutty GA. High-resolution histologic analysis of the human choroidal vasculature. Invest Ophthalmol Vis Sci. 1994; 35:3799–3811. [PubMed: 7928177]
18. Lutty GA, Cao J, McLeod DS. Relationship of polymorphonuclear leukocytes to capillary dropout in the human diabetic choroid. Am J Pathol. 1997; 151:707–714. [PubMed: 9284819]
19. Cao J, McLeod S, Merges CA, et al. Choriocapillaris degeneration and related pathologic changes in human diabetic eyes. Arch Ophthalmol. 1998; 116:589–597. [PubMed: 9596494]
20. Gerl VB, Bohl J, Pitz S, et al. Extensive deposits of complement C3d and C5b-9 in the choriocapillaris of eyes of patients with diabetic retinopathy. Invest Ophthalmol Vis Sci. 2002; 43:1104–1108. [PubMed: 11923252]
21. Stitt AW, Gardiner TA, Archer DB. Histological and ultrastructural investigation of retinal microaneurysm development in diabetic patients. Br J Ophthalmol. 1995; 79:362–367. [PubMed: 7742285]
22. Arend O, Wolf S, Jung F, et al. Retinal microcirculation in patients with diabetes-mellitus: Dynamic and morphological analysis of perifoveal capillary network. British Journal of Ophthalmology. 1991; 75:514–518. [PubMed: 1911651]
23. Matsunaga D, Yi J, De Koo L, et al. Optical coherence tomography angiography of diabetic retinopathy in human subjects. Ophthalmic Surg Lasers Imaging Retina. 2015; 46:796–805. [PubMed: 26431294]
24. Lutty GA. Effects of diabetes on the eye. Investigative Ophthalmology & Visual Science. 2013; 54:ORSF81–ORSF87. [PubMed: 24335073]
25. Hidayat AA, Fine BS. Diabetic Choroidopathy. Ophthalmology. 92:512–522.
26. Shiragami C, Shiraga F, Matsuo T, et al. Risk factors for diabetic choroidopathy in patients with diabetic retinopathy. Graefe's Archive for Clinical and Experimental Ophthalmology. 2002; 240:436–442.
27. Hua R, Liu L, Wang X, et al. Imaging Evidence of Diabetic Choroidopathy In Vivo: Angiographic Pathoanatomy and Choroidal-Enhanced Depth Imaging. Plos One. 2013; 8:e83494. [PubMed: 24349522]

28. Bischoff P, Flower R. Ten years experience with choroidal angiography using indocyanine green dye: a new routine examination or an epilogue? Documenta Ophthalmologica. 1985; 60:235–291. [PubMed: 2414083]
29. Flower RW. Extraction of choriocapillaris hemodynamic data from ICG fluorescence angiograms. Investigative Ophthalmology & Visual Science. 1993; 34:2720–2729. [PubMed: 8344794]
30. Fingler J, Schwartz D, Yang CH, et al. Mobility and transverse flow visualization using phase variance contrast with spectral domain optical coherence tomography. Optics Express. 2007; 15:12636–12653. [PubMed: 19550532]
31. Mariampillai A, Standish BA, Moriyama EH, et al. Speckle variance detection of microvasculature using swept-source optical coherence tomography. Optics Letters. 2008; 33:1530–1532. [PubMed: 18594688]
32. Jia YL, Tan O, Tokayer J, et al. Split-spectrum amplitude-decorrelation angiography with optical coherence tomography. Optics Express. 2012; 20:4710–4725. [PubMed: 22418228]
33. Huang Y, Zhang Q, Thorell MR, et al. Swept-source OCT angiography of the retinal vasculature using intensity differentiation based OMAG algorithms. Ophthalmic surgery, lasers & imaging retina. 2014; 45:382–389.
34. Matsunaga D, Yi J, Puliafito C, et al. OCT angiography in healthy human subjects. Ophthalmic Surg Lasers Imaging Retina. 2014; 45:510–515. [PubMed: 25423629]
35. Kurokawa K, Sasaki K, Makita S, et al. Three-dimensional retinal and choroidal capillary imaging by power Doppler optical coherence angiography with adaptive optics. Optics Express. 2012; 20:22796–22812. [PubMed: 23037430]
36. Braaf B, Vienola KV, Sheehy CK, et al. Real-time eye motion correction in phase-resolved OCT angiography with tracking SLO. Biomed Opt Express. 2013; 4:51–65. [PubMed: 23304647]
37. Kim DY, Fingler J, Zawadzki RJ, et al. Optical imaging of the chorioretinal vasculature in the living human eye. Proc Natl Acad Sci U S A. 2013; 110:14354–14359. [PubMed: 23918361]
38. Choi W, Mohler KJ, Potsaid B, et al. Choriocapillaris and choroidal microvasculature imaging with ultrahigh speed OCT angiography. Plos One. 2013; 8:e81499. [PubMed: 24349078]
39. Kim DY, Fingler J, Zawadzki RJ, et al. Noninvasive imaging of the foveal avascular zone with high-speed, phase-variance optical coherence tomography. Investigative Ophthalmology & Visual Science. 2012; 53:85–92. [PubMed: 22125275]
40. Schwartz DM, Fingler J, Kim DY, et al. Phase-variance optical coherence tomography: a technique for noninvasive angiography. Ophthalmology. 2014; 121:180–187. [PubMed: 24156929]
41. Ishibazawa A, Nagaoka T, Takahashi A, et al. Optical coherence tomography angiography in diabetic retinopathy: A prospective pilot study. American Journal of Ophthalmology. 2015; 160:35–44.e1. [PubMed: 25896459]
42. Choi W, Potsaid B, Jayaraman V, et al. Phase-sensitive swept-source optical coherence tomography imaging of the human retina with a vertical cavity surface-emitting laser light source. Optics Letters. 2013; 38:338–240. [PubMed: 23381430]
43. Unterhuber A, Povazay B, Hermann B, et al. In vivo retinal optical coherence tomography at 1040 nm-enhanced penetration into the choroid. Optics Express. 2005; 13:3252–3258. [PubMed: 19495226]
44. Guizar-Sicairos M, Thurman ST, Fienup JR. Efficient subpixel image registration algorithms. Optics Letters. 2008; 33:156–158. [PubMed: 18197224]
45. Chan G, Balaratnasingam C, Yu PK, et al. Quantitative morphometry of perifoveal capillary networks in the human retinaperifoveal capillary networks. Investigative Ophthalmology & Visual Science. 2012; 53:5502–5514. [PubMed: 22815351]
46. Moore J, Bagley S, Ireland G, et al. Three dimensional analysis of microaneurysms in the human diabetic retina. Journal of Anatomy. 1999; 194:89–100. [PubMed: 10227670]
47. Agemy SA, Scripsema NK, Shah CM, et al. Retinal vascular perfusion density mapping using optical coherence tomography angiography in normals and diabetic retinopathy patients. RETINA. 2015; 35:2353–2363. [PubMed: 26465617]

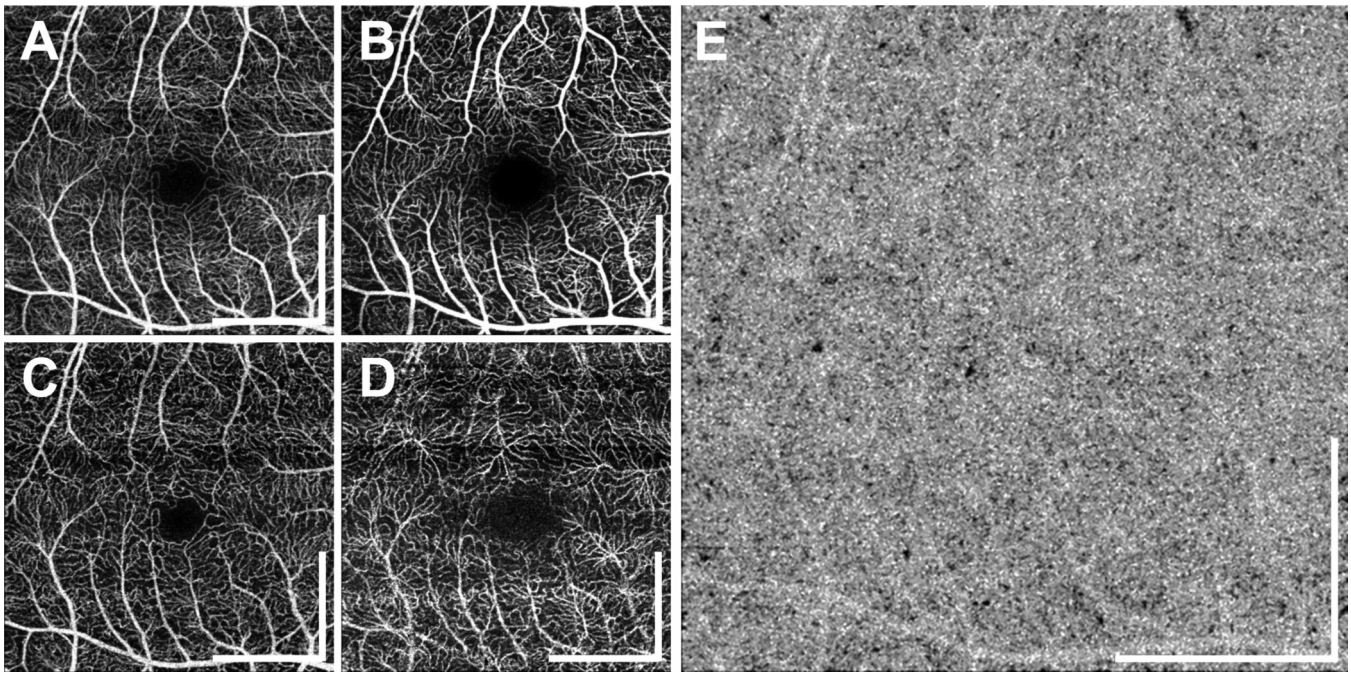

Figure 1.

Retinal vasculature of a 33 year old normal subject. (A) En face OCTA projection through the depths of the entire retinal vasculature (i.e., through all retinal plexuses). The volumes in (A–D) correspond to 3 mm × 3 mm fields. (B–D) En face OCTA of the superficial, intermediate, and deep capillary plexuses. Retinal vasculatures at different depths show distinct patterns. At all depths, the retinal capillary network is dense and ordered. All scale bars: 1 mm. OCTA, optical coherence tomography angiography

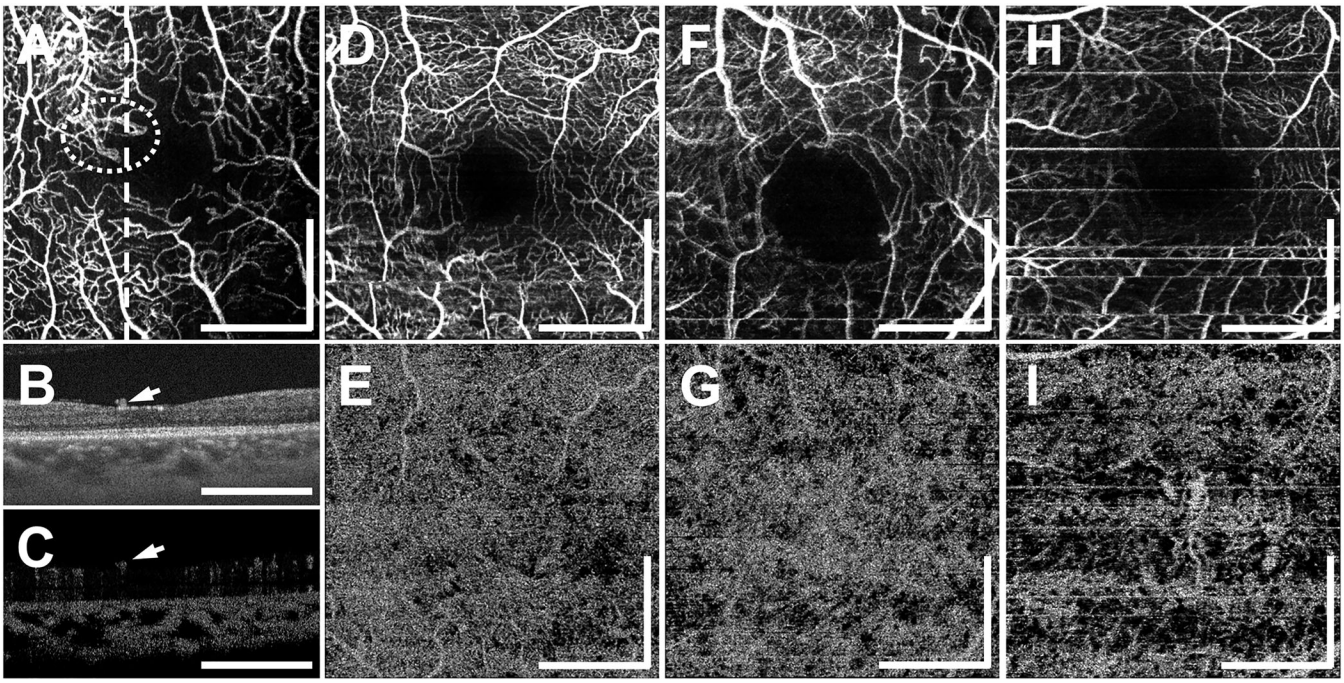

Figure 2.

(A–C) OCT and OCTA images from a 26 year old PDR patient. All en face OCTA images (A, D, F, H) are formed by projecting the OCTA volume through the depths of the entire retinal vasculature (i.e., through all retinal plexuses).(A) En face OCTA projection; the white dotted circle indicates a location of abnormal vasculature. The OCT cross-section (B) and corresponding OCTA cross-section (C), at the position of the dashed white line in (A), clearly show abnormal vasculature above the ILM, as indicated by white arrows. The OCTA signal seen in the outer retina in (C) is an artifact caused by decorrelation tails of the OCTA signal generated from overlying retinal vasculature. (D–E) En face OCTA from a 56 year old PDR patient. The horizontal white lines are artifacts caused by patient motion artifacts. (D) OCTA of the retinal vasculature, and (E) CC slab. (F–G) En face OCTA from a 60 year old PDR patient. (F) OCTA of the retinal vasculature, and (G) CC slab. (H–I) En face OCTA from a 65 year old PDR patient. (H) OCTA of the retinal vasculature, and (I) CC slab. The OCTA CC slabs of (E), (G), and (I) show varying degrees CC flow impairment. All images are 3 mm × 3 mm fields. All scale bars: 1 mm. OCT, optical coherence tomography; OCTA, optical coherence tomography angiography; PDR, proliferative diabetic retinopathy; ILM, inner limiting membrane; CC, choriocapillaris

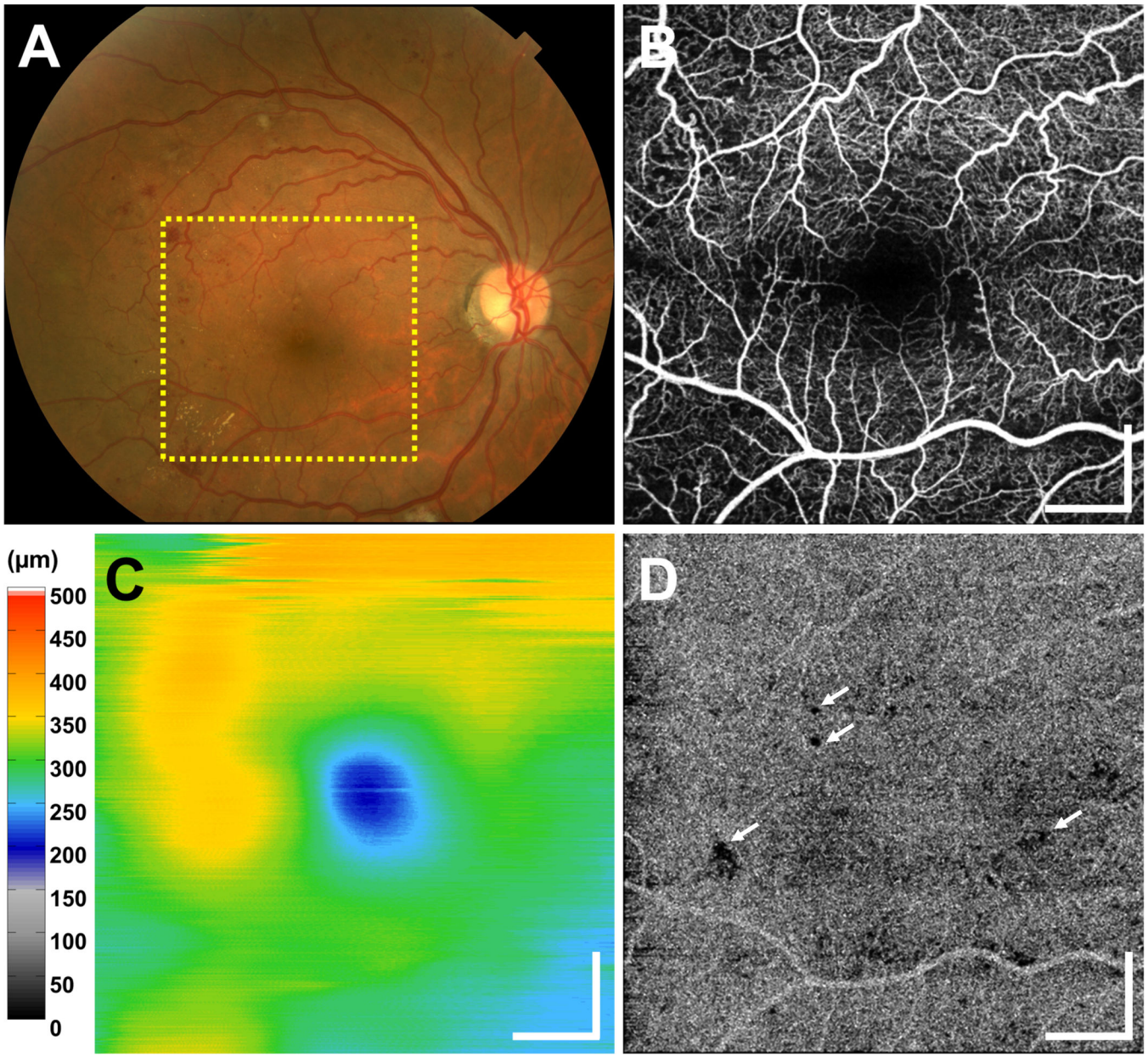

Figure 3.

(A) Fundus photograph and (B–D) OCT and OCTA from a 51 year old NPDR patient with DME. (B) En face OCTA projection through the depths of the entire retinal vasculature (i.e., through all retinal plexuses) reveals vascular remodeling, abnormally tortuous capillary segments at multiple fundus locations, FAZ enlargement, and capillary dropout at several locations in the field of view. (C) Retinal thickness map shows edema. (D) En face OCTA CC slab exhibits several areas of focal CC flow impairment (white arrows point to several such examples), but an otherwise dense and homogenous pattern. OCT and OCTA data acquired from a 6 mm × 6 mm field. All scale bars: 1 mm. OCT, optical coherence tomography; OCTA, optical coherence tomography angiography; NPDR, non-proliferative

diabetic retinopathy; DME, diabetic macular edema; FAZ, foveal avascular zone; CC, choriocapillaris

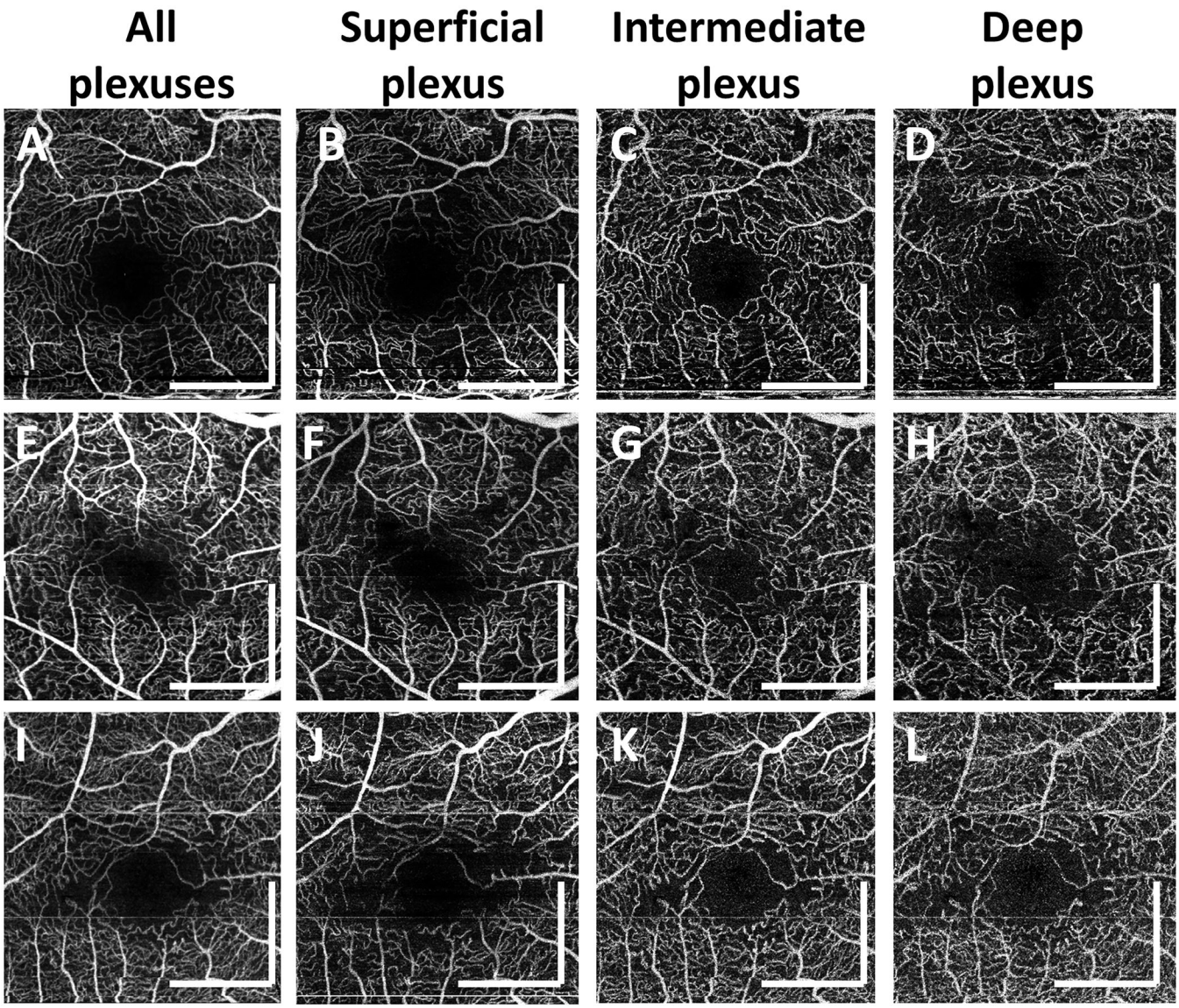

Figure 4.

En face OCTA images from (A–D) 51 year old, (E–H) 63 year old, and (I–L) 64 year old NPDR patients with DME. Separately visualizing en face OCTA images of the superficial, intermediate, and deep capillary plexuses facilitates detection of vascular abnormalities. OCTA images are manually motion corrected for clarity. All images acquired from 3 mm × 3 mm fields. All scale bars: 1 mm. OCTA, optical coherence tomography angiography; NPDR, non-proliferative diabetic retinopathy; DME, diabetic macular edema

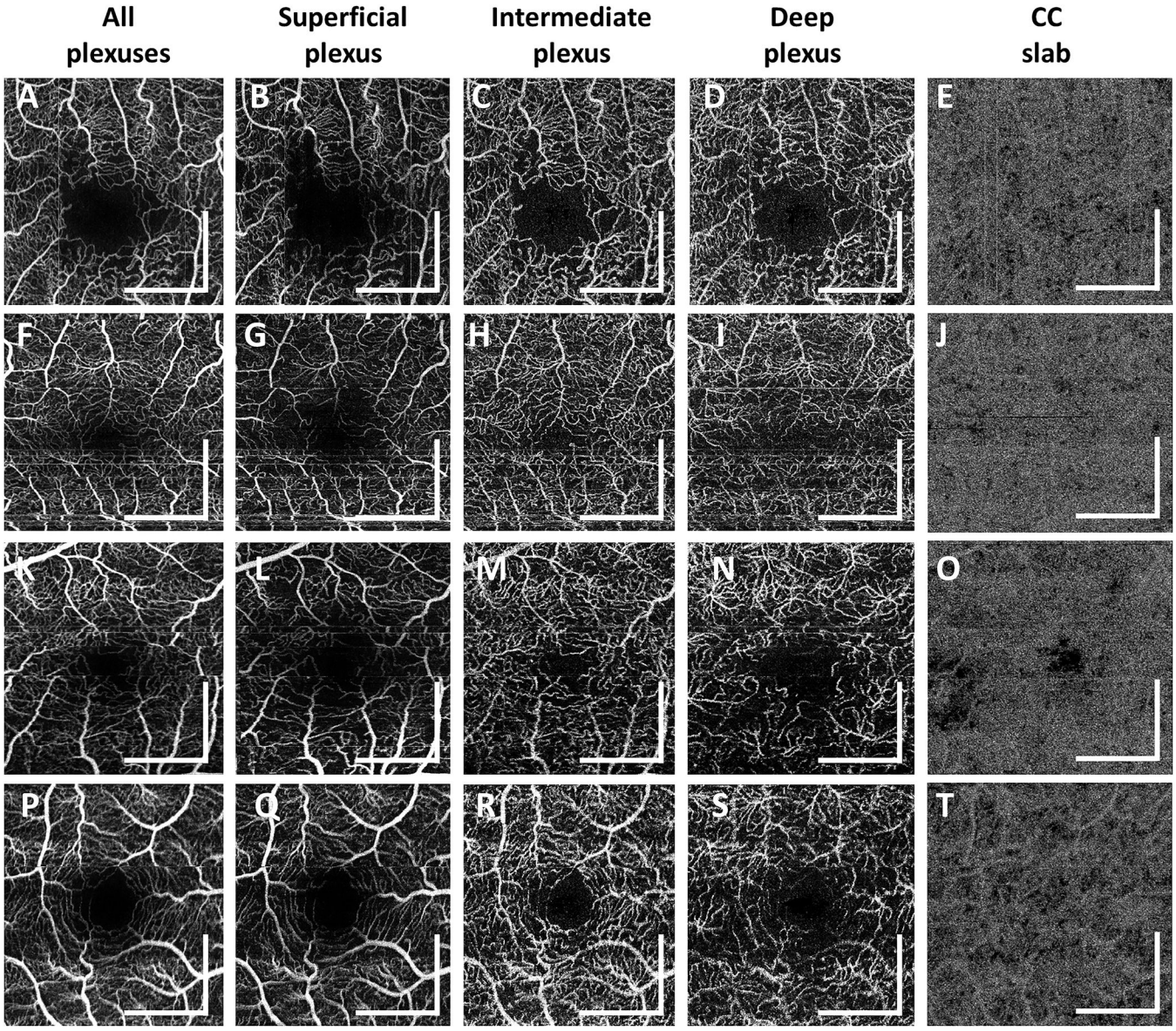

Figure 5.

En face OCTA images from 4 representative diabetic patients without retinopathy. (A–E) 64 year old diabetic patient. (F– J) 68 year old diabetic patient. (K–O) 68 year old diabetic patient. (P–T) 68 year old diabetic patient. (A,F,K,P) En face OCTA projection through the depths of the entire retinal vasculature (i.e., through all retinal plexuses). (B, G, L, Q) En face OCTA projection through the depths spanned by the superficial plexus. (C, H, M, R) En face OCTA projection through the depths spanned by the intermediate plexus. (D, I, N, S) En face OCTA projection through the depths spanned by the deep plexus. (E, J, O, T) Corresponding OCTA CC slabs. All images are 3 mm × 3 mm fields. En face retinal OCTA images were manually motion corrected for clarity. All scale bars: 1mm. OCTA, optical coherence tomography angiography; CC, choriocapillaris

Table 1

Subject characteristics.

	Subjects imaged	Eyes imaged	Age ± std. (years)	Sex (males; females)	Race (African; Asian; Caucasian; Hispanic)
Normal subjects	32	63	40.7 ± 14.1	13; 19	3; 4; 25
DM without DR	28	51	59.7 ± 13.2	17; 11	6; 10; 11; 1
NPDR	16	29	60.8 ± 7.4	9; 7	5; 2; 9; 0
PDR	7	9	51.4 ± 16.3	3; 4	1; 1; 5; 0
Total	82	152			